THE JOURNAL OF PHYSICAL CHEMISTRY C

ARTICLE

pubs.acs.org/JPCC

Enhanced Fano Resonance in Asymmetrical Au:Ag Heterodimers

O. Peña-Rodríguez,*,† U. Pal,‡ M. Campoy-Quiles,† L. Rodríguez-Fernández,§ M. Garriga,† and M. I. Alonso†

†Institut de Ciència de Materials de Barcelona (ICMAB-CSIC), Campus UAB, Bellaterra, Barcelona 08193, Spain

‡Instituto de Física, Universidad Autónoma de Puebla, Apartado Postal J-48, Puebla, Puebla 72570, Mexico

§Instituto de Física, Universidad Nacional Autónoma de México, Apartado Postal 20-364, México D.F. 01000, Mexico

ABSTRACT: The geometrical configuration of Au:Ag nanoparticle heterodimers can be optimized to produce prominent Fano resonance (FR) signals, strong enough to be detectable by standard spectroscopic techniques. The highest intensity of the FR in these bimetallic dimers is reached when the size ratio of the nanoparticles (R_{Au}:R_{Ag}) is close to 3:1. Moreover, the FR can be induced only by the longitudinal component of the dimer surface plasmon resonance (SPR). Finally, it is found that the sensitivity of the dimer FR signal to the variation in the refractive index of the surrounding medium (n_m) is 2 times larger than that of the associated SPR for the region where $n_m < 1.5$, which opens up the possibility of utilizing the FR band for more efficient optical sensing applications.

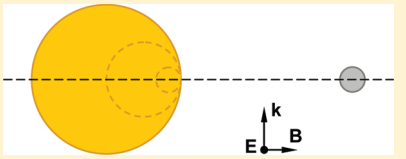

INTRODUCTION

The study of the optical properties of metallic nanoparticles (NPs) has attracted increased interest in recent years,[1,2] mainly due to the many potential applications of the resonant oscillation of the free electrons in metal surfaces, a phenomenon known as surface plasmon resonance (SPR). Sensing,[3,4] medicine,[5] catalysis,[6] optoelectronics,[7,8] solar energy conversion,[9,10] and even as "nanorulers",[11,12] the list of prospective applications based on the SPR of metal nanoparticles is ever increasing. However, a precise control of the SPR intensity and position is required in order to optimize the NPs for each particular application. SPR can be controlled either through changes in geometrical factors such as size and shape[13] or by forming NP aggregates,[14−16] where the optical properties of the ensemble are strongly modified.

It is striking that the simplest possible aggregate, the dimer, has proved to be one of the most interesting, not only as a prototype to study electromagnetic phenomena occurring in the aggregates,[17] but also for practical applications such as the nanoruler.[18] Numerous theoretical and experimental studies[17−24] have been made on such systems. Though homodimers have been more widely studied, the effects of variations in size and/or composition of the constituent particles have been also investigated, to a lesser extent. In the latter case, due to the heterogeneity in size and/or composition, a variety of new properties could be observed.[19−22] One of them, recently discovered for the size-symmetrical Au:Ag heterodimer, is the all-plasmonic Fano resonance (FR),[19] arising from the coupling between the SPR of the Ag NP and the continuum of interband transitions of the Au NP. In this respect, it should be clarified that talking about the SPR of the individual particles in the dimer is not strictly correct, because what we have actually are two eigenmodes of the entire system.[17] However, it is a common practice in the FR-related literature (to which we adhere in this paper) to refer to the high- and low-energy SPR modes of the Au:Ag dimer as "silver SPR" and "gold SPR" modes because they are mainly derived from the SPR of silver and gold, respectively.

Unfortunately, the Fano profiles discovered by Bachelier et al.[19] were masked by the intense peak of the silver SPR, complicating their experimental detection. Though the intensity of Fano resonance rises by increasing the size of silver particle,[19] its detection becomes even harder due to the stronger increase of SPR peak intensity. It was also demonstrated recently that the Fano resonances can be obtained in the asymmetric gold dimer.[21] However, these profiles are far from optimal, because the Au SPR peak is not as narrow as that of Ag.

In this work, we have theoretically studied, by means of T-matrix calculations,[25] the optical properties of asymmetrical Au:Ag heterodimers for different size ratios of the nanoparticles. We found an optimum configuration for enhancing the Fano resonances for the dimer with a size ratio (R_{Au}:R_{Ag}) close to 3:1. For this setting, we obtained a clear Fano resonance which was not hidden by the silver SPR whereas, at the same time, it was strong enough to be detected experimentally. Dependence of the SPR and FR on the refractive index of the host matrix is also analyzed and we find that the FR is roughly twice more sensitive to the changes in the environment than the SPR, which makes the former more suitable than the latter for sensing applications.

PROCEDURE

In this work, we have focused on finding configurations of Au:Ag heterodimers with a Fano resonance as large as possible, so that it can be experimentally detected. As has been mentioned above, the symmetric heterodimer does not meet this condition because the intense SPR peak hides the Fano profile. Increasing the size of the Au particle enhances its contribution to the optical spectrum of the dimer ensemble until, beyond some size ratio, the Fano resonance becomes visible. However, at some point the relative size of the Ag particle would be so small that its contribution to the dimer spectrum would be negligible. This suggests that there must be some optimal configuration for which the intensity of the Fano resonance would be maximized.

Received: January 17, 2011
Revised: February 22, 2011
Published: March 11, 2011

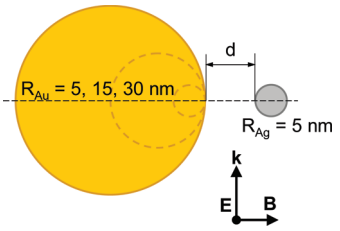

Figure 1. Schematic representation of the studied asymmetrical Au:Ag heterodimer. **E** and **B** are the electric and magnetic fields, respectively and **k** is the wave vector.

Taking the above possibilities into consideration, we have theoretically investigated different types of asymmetrical heterodimers, as shown in Figure 1, to find the optimum configuration. Here, we will present three specific cases, where the radius of the Ag particle was kept constant (R_{Ag} = 5 nm) and the radius of the gold particle varied (R_{Au} = 5, 15, 30 nm). Additionally, the optical extinction spectra of four other configurations (R_{Ag}[nm]:R_{Au}[nm] of 10:30, 15:45, 20:60, and 25:75) were calculated, in order to analyze the variations of the FR with the increase of the dimer size. Our calculations were carried out using the free T-matrix code developed by Mackowski, Fuller, and Mishchenko.[26,27] The bulk dielectric function values of gold and silver reported by Johnson and Christy[28] were used here, after applying a size correction that incorporates the surface dispersion effects.[29] Except otherwise specified, the calculations were performed for dimers immersed in water (n_m = 1.33).

Now, a word of warning concerning the studied configurations is in order here. Recent experimental evidence[12] suggests that for silver dimers with a ratio of center-to-center separation to effective diameter, $(R_{Au} + R_{Ag} + d)/(R_{Au} + R_{Ag})$, below 1.05 the plasmon coupling does not continue to intensify with decreasing interparticle separation. There are only three configurations in our work below this limit: [R_{Au}, R_{Ag}, d] = [30, 5, 1], [60, 20, 3], and [75, 25, 3], but a deviation of these points would not alter our conclusions; therefore, we are confident in the validity of our results. Note, however, that to synthesize dimers based on our results this additional constraint should be taken into account to avoid systems where the SPR coupling (and therefore the FR) might be reduced by the mentioned effect.[12]

The individual contribution of each particle to the total extinction efficiency (Q_{ext}) was also calculated, in order to achieve a more accurate interpretation of the obtained results. The relation between the extinction efficiency and the corresponding cross section is $\sigma_{ext} = AQ_{ext}$, where A is the geometrical cross section of the particle/ensemble. The extinction cross section of the dimer ($\sigma_{ext}^{Au:Ag}$) is equal to the sum of the extinction cross sections of both particles (σ_{ext}^{Au} and σ_{ext}^{Ag}):[26,30]

$$\sigma_{ext}^{Au:Ag} = \sigma_{ext}^{Au} + \sigma_{ext}^{Ag} \quad (1)$$

Then

$$Q_{ext}^{Au:Ag} = Q_{ext}^{Au}\frac{R_{Au}^2}{R_{Au:Ag}^2} + Q_{ext}^{Ag}\frac{R_{Ag}^2}{R_{Au:Ag}^2} \quad (2)$$

where $R_{Au:Ag} = (R_{Au}^3 + R_{Ag}^3)^{1/3}$ is the volume-equivalent radius of the dimer (i.e., the radius of a sphere having the same volume) and both terms of the summation can be interpreted as the partial contribution to the total extinction efficiency of Au and Ag ($\langle Q_{ext}^{Au} \rangle$ and $\langle Q_{ext}^{Ag} \rangle$), respectively.

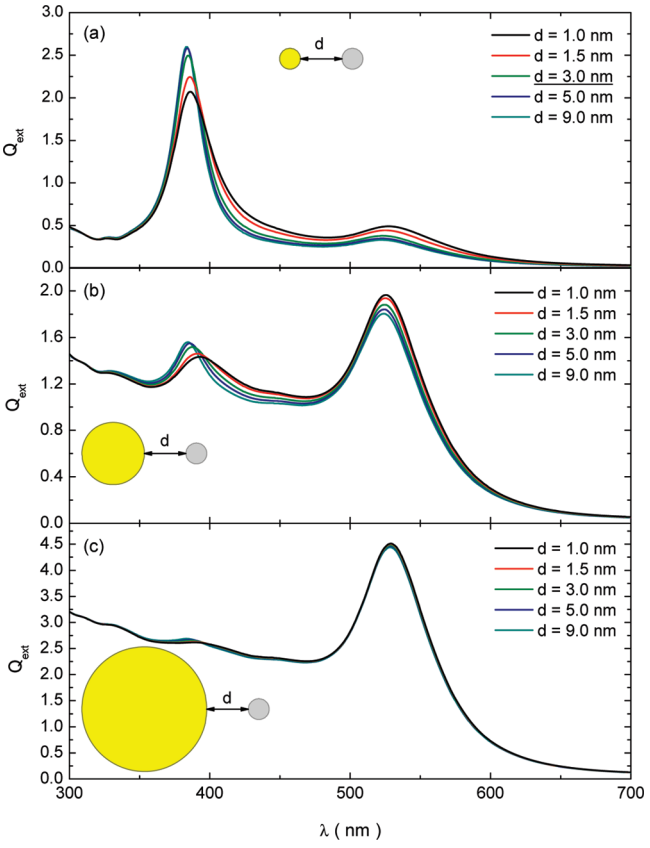

Figure 2. Simulated optical extinction spectra (using unpolarized light) for the Au:Ag heterodimers with R_{Au}:R_{Ag} ratios of (a) 1:1, (b) 3:1, and (c) 6:1, and different interparticle separations, embedded within a matrix with refractive index n_m = 1.33. The underlined configuration corresponds to the one studied in ref 19.

RESULTS AND DISCUSSION

The extinction spectra of Au:Ag dimers as a function of the surface-to-surface distance (d), with a constant R_{Ag} (5 nm) and varying R_{Au} (5, 15, 30 nm), are shown in Figure 2. The first case (Figure 2a) coincides with the dimer studied by Bachelier et al.[19] (the actual configuration, d = 3 nm, is underlined), included here for comparison. The spectra are characterized by two bands, located around 390 and 540 nm, which correspond to a combined FR-Ag SPR and the Au SPR, respectively. For shorter d values both peaks red shift as a result of the stronger coupling between the SPR of the individual particles. As already mentioned, the FR cannot be clearly traced in this system due to the presence of the intense Ag SPR peak. However, the extinction spectra change markedly for the next studied dimer (R_{Ag} = 5 nm, R_{Au} = 15 nm; Figure 2b). First, we can observe that the red shift of the low-energy peak is smaller than in the previous case. Moreover, a clear Fano profile can be observed at the position corresponding to the high-energy SPR peak, especially for the configurations with the shorter d values. Then, on increasing the interparticle distance, this high-energy peak blue-shifts and acquires a more "SPR-like" shape. Finally, for the configuration with R_{Au} = 30 nm (Figure 2c), the extinction spectrum hardly changes on varying d, suggesting that the silver particle is too small to affect the extinction spectrum of gold significantly.

Figure 3 shows the contribution of each individual particle to the total extinction spectrum, calculated for all three configurations

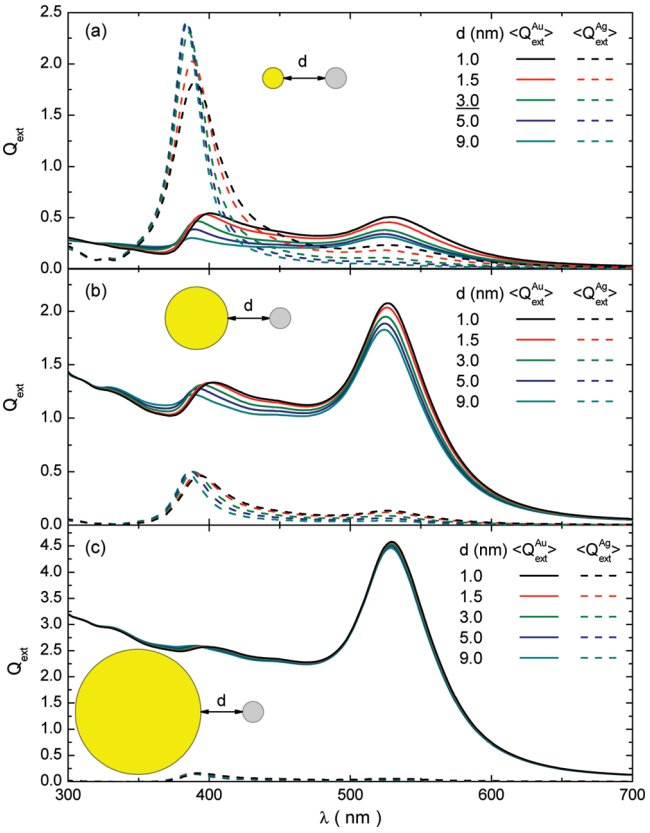

Figure 3. Contributions of the Au (solid lines) and Ag particles (dashed lines) to the optical extinction spectra of the Au:Ag heterodimers, for unpolarized light incidence. The spectra were calculated for dimers with R_{Au}:R_{Ag} ratios of (a) 1:1, (b) 3:1, and (c) 6:1, and different interparticle (surface-to-surface) distances. The refractive index of the surrounding matrix is n_m = 1.33. The underlined configuration corresponds to the one studied in ref 19.

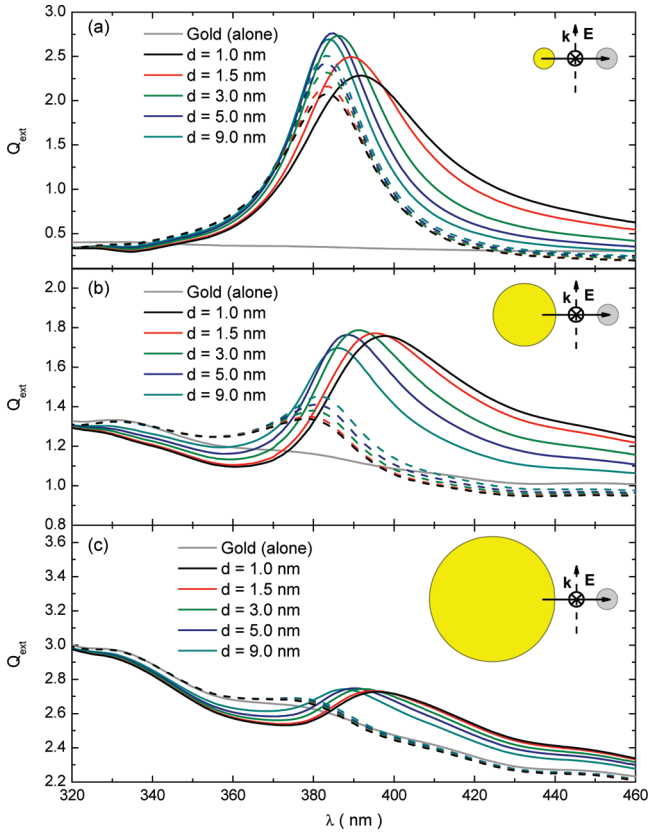

Figure 4. Simulated optical extinction spectra for the Au:Ag heterodimers with R_{Au}:R_{Ag} ratios of (a) 1:1, (b) 3:1, and (c) 6:1, and different interparticle separations (surface-to-surface distances) embedded within a matrix with refractive index n_m = 1.33. The spectra were calculated for excitations parallel (solid curves) and perpendicular (dashed curves) to the dimer axis. **E** represents the incident electric field and **k** is the wave vector, here entering into the paper sheet.

(see eq 2) studied here. In the case of the symmetrical heterodimer (Figure 3a), it is confirmed that the silver SPR is more intense than the Fano resonance (for the comparison we have taken the intensity of the FR to be the difference between the maximum and the minimum of the oscillation). However, for the 3:1 ratio (Figure 3b) the FR is not obscured by the silver SPR because they have similar intensities. The FR, however, appears to be shifted toward lower wavelengths due to the contribution of the silver SPR. Finally, when the size of the silver particle (and therefore its SPR) is much smaller than the Au one (third case; Figure 3c), the intensity of the induced Fano resonance is weak, making its detection as complicated as in the first case. Therefore, it is clear that the FR can be detected more easily when the relationship R_{Au}:R_{Ag} is close to 3:1, even if it appears displaced due to the presence of the silver SPR.

The optical extinction spectra of the heterodimers were also calculated for linearly polarized light (Figure 4). Two different polarizations were used: parallel (solid lines) and perpendicular (dashed lines) to the axis of the dimer. Interestingly, Figure 4 shows that, irrespective of d, there is little trace of the FR for perpendicularly polarized light. Only the SPR peak appears in the spectra and it blue-shifts with the decrease of interparticle distance, as we would expect in the absence of the Fano effect. However, for parallel polarization the spectra change dramatically; for all size ratios, including R_{Au}:R_{Ag} = 1:1. Two important effects could be observed. First, the shape and position of the profiles (more prominent for R_{Au}:R_{Ag} = 3:1; Figure 4b) correspond to that of the Fano resonances that would be observed if only the gold particle is excited (Figure 3). Second, on decreasing d the resonance red-shifts, in contrast to what is observed for perpendicular polarization. All these observations suggest that the Fano resonance is induced only by the longitudinal component of the silver SPR. This behavior can be rationalized since for the transverse polarization the electrons in each particle oscillate independently, with little interaction between the adjacent spheres, whereas for longitudinal excitation the interparticle interaction is much stronger.

So far we have performed the calculations using small particle sizes, in order to avoid the higher-order resonances and simplify the analysis. However, as has been demonstrated below, the obtained results hold for larger particles too. The optical extinction spectra, calculated for the heterodimer with R_{Au}:R_{Ag} = 3:1 and d = 3.0 nm and using linearly light polarized parallel to the dimer axis, are shown in Figure 5a. We can see that on increasing the dimer size the FR intensity increases. This behavior changes when the silver particle becomes so large that the phase retardation effects give rise to the quadrupolar SPR. In this case the dipolar Fano resonance becomes more diffuse (because the dipolar Ag SPR is wider) and a new, weaker but clear enough, FR related to the quadrupolar SPR peak appears. Our calculations

dx.doi.org/10.1021/jp200495x |J. Phys. Chem. C 2011, 115, 6410–6414

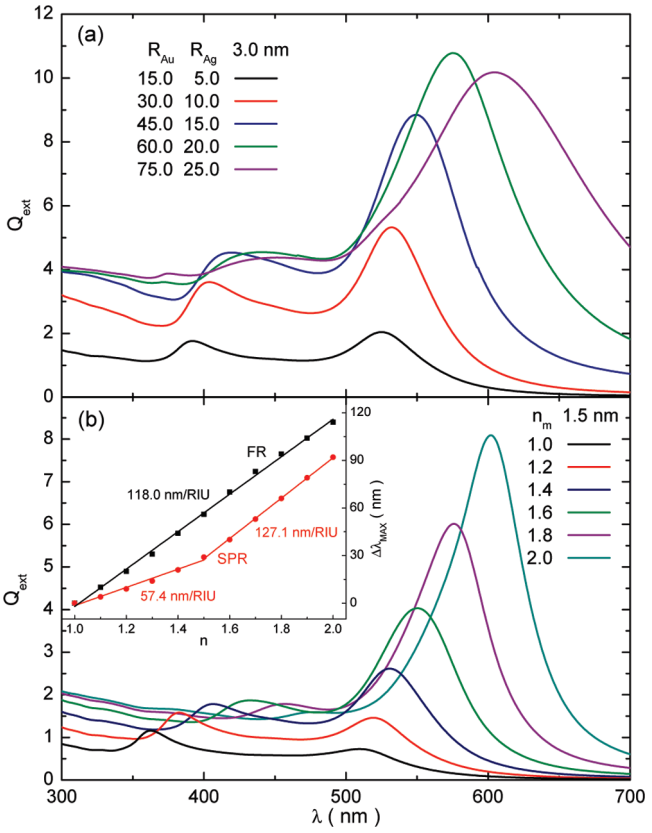

Figure 5. Simulated optical extinction spectra for the R_{Au}:R_{Ag} = 3:1 heterodimer (a) increasing the size with fixed parameters n_m = 1.33 and d = 3.0 nm and (b) increasing the refractive index of the matrix (n_m in [1.0, 2.0]) with d = 1.5 nm. The inset shows the variation of the FR (black squares) and the SPR (red circles) positions as a function of the refractive index of the matrix. The lines in the inset are linear fits to the data.

(not shown here) indicate that the previously obtained optimal size ratio (3:1) is also valid for larger dimers, at least for R_{Au} < 100 nm. For dimers greater than this size the optical extinction spectrum becomes more complex and the FR cannot be seen as clearly as for smaller NP sizes independently of the size ratio.

Finally, the effect of the surrounding medium on the extinction spectra of the dimers is also studied (Figure 5b). The calculations were performed using light polarized parallel to the dimer axis for the configuration with highest sensitivity, that is, R_{Au}:R_{Ag} = 3:1. Though an arbitrary interparticle separation of d = 1.5 nm was chosen for these calculations, similar results can be obtained also for other values (not shown). Both the FR and the SPR red shift upon increasing the matrix refractive index but the former is more sensitive than the latter (see the inset on Figure 5b). The FR sensitivity ($\Delta\lambda/\Delta n_m$), in nanometers per refractive index units (RIU), is approximately linear in the whole range (118.0 nm/RIU) but for the SPR we can distinguish two regimes. For n_m < 1.5, i.e., most liquids, the SPR has a low sensitivity (57.4 nm/RIU) which is roughly half of that of the FR while for greater values of n_m the SPR sensitivity increases (127.1 nm/RIU) until both of them become approximately equal. The obtained results indicate that for most practical cases (namely, for n_m below 1.5) it would be more convenient to use the FR for optical sensing applications instead of the more commonly used SPR. Clearly, further works (both theoretical and experimental), which are out of the scope of this paper, are needed in order to exploit this interesting property of heterodimers for technological applications. For example, factors such as the intensity and the spectrum width of the Fano resonance should be discussed in more detail to determine whether or not the FR is actually better than the SPR for sensing applications.

CONCLUSIONS

Plasmonic Fano resonances in asymmetrical Au:Ag heterodimers have been studied as a function of the nanoparticles' size ratio and interparticle separation. The geometrical configuration of the dimers can be optimized to achieve intense Fano profiles, detectable by standard spectroscopic techniques. A size ratio of the individual particles R_{Au}:R_{Ag} close to 3:1 and shorter interparticle separations produce stronger Fano resonance signals. The Fano profile is particularly prominent in the extinction spectra when the dimers are excited by linearly polarized light, parallel to the longitudinal axis. The FR is twice as sensitive as the associated SPR to changes in the refractive index of the surrounding medium for n_m values below 1.5. Moreover, the sensitivity of the FR has a more linear behavior than its SPR counterpart. The results obtained in this work open up the advantageous possibility of using the FR band for optical sensing applications instead of (or together with) the conventional SPR peak.

AUTHOR INFORMATION

Corresponding Author

*E-mail: ovidio@bytesfall.com.

ACKNOWLEDGMENT

O.P.R. thanks DGAPA-UNAM and ICMAB-CSIC for extending a postdoctoral fellowship through the UNAM-CSIC agreement. M.C.Q. is grateful to the Spanish Ministry of Science for a "Ramón y Cajal" fellowship.

REFERENCES

(1) Barnes, W. L.; Dereux, A.; Ebbesen, T. W. Surface plasmon subwavelength optics. *Nature* **2003**, *424*, 824–830.

(2) Maier, S. A.; Kik, P. G.; Atwater, H. A.; Meltzer, S.; Harel, E.; Koel, B. E.; Requicha, A. A. Local detection of electromagnetic energy transport below the diffraction limit in metal nanoparticle plasmon waveguides. *Nat. Mater.* **2003**, *2*, 229–232.

(3) Alivisatos, P. The use of nanocrystals in biological detection. *Nat. Biotechnol.* **2004**, *22*, 47–52.

(4) Sun, Y.; Xia, Y. Increased sensitivity of surface plasmon resonance of gold nanoshells compared to that of gold solid colloids in response to environmental changes. *Anal. Chem.* **2002**, *74*, 5297–5305.

(5) Hirsch, L. R.; Stafford, R. J.; Bankson, J. A.; Sershen, S. R.; Rivera, B.; Price, R. E.; Hazle, J. D.; Halas, N. J.; West, J. L. Nanoshell-mediated near-infrared thermal therapy of tumors under magnetic resonance guidance. *Proc. Natl. Acad. Sci. U.S.A.* **2003**, *100*, 13549–13554.

(6) Tihay, F.; Pourroy, G.; Richard-Plouet, M.; Roger, A. C.; Kiennemann, A. Effect of Fischer−Tropsch synthesis on the microstructure of Fe-Co-based metal/spinel composite materials. *Appl. Catal., A* **2001**, *206*, 29–42.

(7) Mazzoldi, P.; Arnold, G. W.; Battaglin, G.; Gonella, F.; Haglund, R. F. Metal nanocluster formation by ion implantation in silicate glasses:. nonlinear optical applications. *J. Nonlinear Opt. Phys. Mater.* **1996**, *5*, 285–330.

(8) Pavesi, L.; Dal Negro, L.; Mazzoleni, C.; Franzo, G.; Priolo, F. Optical gain in silicon nanocrystals. *Nature* **2000**, *408*, 440–444.
(9) Kamat, P. V.; Schatz, G. C. Nanotechnology for next generation solar cells. *J. Phys. Chem. C* **2009**, *113*, 15473–15475.
(10) Atwater, H. A.; Polman, A. Plasmonics for improved photovoltaic devices. *Nat. Mater.* **2010**, *9*, 205–213.
(11) Reinhard, B. M.; Siu, M.; Agarwal, H.; Alivisatos, A. P.; Liphardt, J. Calibration of dynamic molecular rulers based on plasmon coupling between gold nanoparticles. *Nano Lett.* **2005**, *5*, 2246–2252.
(12) Yang, L.; Wang, H.; Yan, B.; Reinhard, B. M. Calibration of silver plasmon rulers in the 1−25 nm separation range: Experimental indications of distinct plasmon coupling regimes. *J. Phys. Chem. C* **2010**, *114*, 4901–4908.
(13) Kelly, K. L.; Coronado, E.; Zhao, L. L.; Schatz, G. C. The optical properties of metal nanoparticles: the influence of size, shape, and dielectric environment. *J. Phys. Chem. B* **2003**, *107*, 668–677.
(14) Xu, Y. Electromagnetic scattering by an aggregate of spheres: far field. *Appl. Opt.* **1997**, *36*, 9496–9508.
(15) Budnyk, A. P.; Damin, A.; Agostini, G.; Zecchina, A. Gold nanoparticle aggregates immobilized on high surface area silica substrate for efficient and clean SERS applications. *J. Phys. Chem. C* **2010**, *114*, 3857–3862.
(16) Lazarides, A. A.; Lance Kelly, K.; Jensen, T. R.; Schatz, G. C. Optical properties of metal nanoparticles and nanoparticle aggregates important in biosensors. *J. Mol. Struct.: THEOCHEM* **2000**, *529*, 59–63.
(17) Nordlander, P.; Oubre, C.; Prodan, E.; Li, K.; Stockman, M. I. Plasmon hybridization in nanoparticle dimers. *Nano Lett.* **2004**, *4*, 899–903.
(18) Chen, J. I. L.; Chen, Y.; Ginger, D. S. Plasmonic nanoparticle dimers for optical sensing of DNA in complex media. *J. Am. Chem. Soc.* **2010**, *132*, 9600–9601.
(19) Bachelier, G.; Russier-Antoine, I.; Benichou, E.; Jonin, C.; Del Fatti, N.; Vallée, F.; Brevet, P. Fano profiles induced by near-field coupling in heterogeneous dimers of Gold and Silver nanoparticles. *Phys. Rev. Lett.* **2008**, *101*, 197401.
(20) Encina, E. R.; Coronado, E. A. On the far field optical properties of Ag-Au nanosphere pairs. *J. Phys. Chem. C* **2010**, *114*, 16278–16284.
(21) Brown, L. V.; Sobhani, H.; Lassiter, J. B.; Nordlander, P.; Halas, N. J. Heterodimers: plasmonic properties of mismatched nanoparticle pairs. *ACS Nano* **2010**, *4*, 819–832.
(22) Sheikholeslami, S.; Jun, Y.; Jain, P. K.; Alivisatos, A. P. Coupling of optical resonances in a compositionally asymmetric plasmonic nanoparticle dimer. *Nano Lett.* **2010**, *10*, 2655–2660.
(23) Hao, E.; Schatz, G. C. Electromagnetic fields around silver nanoparticles and dimers. *J. Chem. Phys.* **2004**, *120*, 357–366.
(24) Xiao, J. J.; Huang, J. P.; Yu, K. W. Optical response of strongly coupled metal nanoparticles in dimer arrays. *Phys. Rev. B* **2005**, *71*, 045404.
(25) Mishchenko, M. I.; Travis, L. D.; Lacis, A. A. *Scattering, absorption, and emission of light by small particles*, 1st ed.; Cambridge University Press: Cambridge, UK, 2002.
(26) Mackowski, D. W. Calculation of total cross sections of multiple-sphere clusters. *J. Opt. Soc. Am. A* **1994**, *11*, 2851–2861.
(27) Mackowski, D. W.; Mishchenko, M. I. Calculation of the T matrix and the scattering matrix for ensembles of spheres. *J. Opt. Soc. Am. A* **1996**, *13*, 2266–2278.
(28) Johnson, P. B.; Christy, R. W. Optical constants of the noble metals. *Phys. Rev. B* **1972**, *6*, 4370.
(29) Hövel, H.; Fritz, S.; Hilger, A.; Kreibig, U.; Vollmer, M. Width of cluster plasmon resonances: Bulk dielectric functions and chemical interface damping. *Phys. Rev. B* **1993**, *48*, 18178.
(30) Bohren, C. F.; Huffman, D. R. *Absorption and scattering of light by small particles*; Wiley-Interscience: New York, 1998.